Surface atomic geometry of Si(001)-(2×1): A low-energy electron-diffraction structure analysis

H. Over,* J. Wasserfall, and W. Ranke
Fritz-Haber-Institut der Max-Planck-Gesellschaft, Faradayweg 4-6, D-14195 Berlin, Germany

C. Ambiatello, R. Sawitzki, D. Wolf, and W. Moritz
Institut für Kristallographie der Universität München, Theresienstrasse 41, D-80333 München, Germany

(Received 23 May 1996)

The reconstruction of the Si(001)-2×1 surface consists of asymmetric and buckled Si dimers. The vertical separation between the up and the down atom within the dimer is about 0.72±0.05 Å and the dimer bond length of 2.24±0.08 Å has been found to be slightly smaller than the Si-Si distance in the bulk. The tilt of the dimer is 19±2°. The formation of Si dimers induces pronounced distortions in the substrate that were detectable down to the fifth Si layer. The structure determination is based on two independent low-energy electron-diffraction data sets taken in two different laboratories. The structural results agree well within the error limits, though noticeable differences occur between the experimental data sets. These differences in the experimental data can possibly be attributed to different preparation procedures. [S0163-1829(97)07807-7]

I. INTRODUCTION

In the recent years, a general consensus has been reached on the principle atomic structure of the clean Si(001)-2×1 surface,[1–7] although accurate structural data of this surface are still missing. The main structural element consists of the formation of Si dimers, which reduces the number of dangling bonds per surface atom from two in the bulk-truncated structure to one in the reconstructed surface, which lowers the surface energy by about 1 eV.[1] In addition, buckled dimers form because the half-filled bands of dangling bonds of a symmetric dimer rearrange themselves into one (more) filled band (associated with the Si up atoms) and one (more) empty band (related to Si down atoms),[1–7] thereby lowering the surface energy further by about 0.1 eV. In the molecular-orbital language, the down atom adopts a planar quasi-sp^2 configuration, while the up atom in the dimer adopts a quasi-p^3 configuration. Experimental evidence for the presence of buckled dimers has been provided by low-energy electron diffraction (LEED), which indicated a reversible transformation of the 2×1 structure into the $c(2\times4)$ phase upon cooling below 200 K.[4] It has been shown that the energy gain associated with this phase transition is on the order of 10 meV.[8] A strong indication of the presence of buckled dimers on the clean Si(001)-2×1 surfaces goes back to photoemission studies[5,9] and scanning tunneling microscopy (STM) spectroscopy,[10] which both demonstrated that the Si(001)-2×1 surface is nonmetallic. With symmetric dimers the Si(001) surface should become metallic; recall that for this configuration the bands associated with the dangling bonds are half filled. In early total-energy calculations,[1,7(a)] the dimers were found to be asymmetric as well as buckled, which produces a surface with semiconducting properties compatible with the above-mentioned experiments. Recent high-resolution photoemission data identified two inequivalent types of surface silicon atoms that were assigned to be the up and down atoms of buckled dimers.[11] Both a rapid flipping between these configurations or a statistical (static) distribution of these buckled dimers would still be conceivable. However, from the antiferromagnetic ordering of the 2×1 phase into the $c(2\times4)$ (Ref. 4) and from recent low-temperature STM,[6] which imaged this phase transition directly, the interpretation of switching dimers is favored over static dimers. More specifically, at room temperature, a large fraction of the surface was covered with apparently symmetric dimers, while on cooling to low temperatures (120 K), an increase of dimers in the asymmetric configuration was observed. Hence the STM images at room temperature, showing symmetric dimer configurations, were argued to be a consequence of time averaging.[6] Corresponding molecular-dynamics calculations supported this view.[12] The dimerization of the topmost Si layer induces, as a consequence, strong local strain fields in the surface region, resulting in displacements of Si atoms in deeper layers.

Complex dynamical LEED analyses were performed, but did not yield compelling evidence of buckled dimers[13–16] since the structural parameters that came out of these analyses scattered too much and the overall agreement between theory and experiment was not very convincing. One possible reason might be seen in the marked variations of experimental LEED data taken at different laboratories, which have been studied carefully by Jona and co-workers.[15,17] An additional attribute of the Si(001)-(2×1) model was introduced by Yang, Jona, and Marcus,[15] which consisted of a twist of the in-plane dimer axis besides the (out-of-plane) tilting. The inclusion of this structural element resulted indeed in a better fit of the experimental LEED data, although the overall agreement between theory and experiment was still not satisfying. The importance of this twist was not shown since it would have necessitated the simultaneous refinement of all important structure parameters that was beyond the capabilities of the LEED program codes and of the computers in those days.

In this work we provide a complete set of crystallographic data of the Si(001)-(2×1) on the basis of two experimental LEED data sets measured in two laboratories. Probably due to different preparation techniques, the experimental data sets are slightly different, an effect that is not uncommon to

LEED studies on the Si(001) surface. The experimental data used in the previous LEED analyses,[13–16] however, have been quite different, although the reason for these differences could not be clearly identified. It has been noticed for a long time that the LEED intensities from Si(001) may change rapidly after preparation[18] probably due to contamination or different states of order induced by small amounts of contamination or by mechanical stress. Also the doping level of the Si samples might exert an appreciable influence on the surface structure since not only the electronic properties are affected, but also structure-related effects such as the bulk diffusion of Li on Si(001).[19] Both data sets presented here agree relatively well compared with the deviations found in the previous studies. The structural data derived from the two data sets are consistent within the error limits. The atomic geometry is also consistent with recent theoretical studies and give strong evidence in favor of the presence of buckled (i.e., asymmetric) dimers on Si(001)-2×1 together with substantial atomic distortions down to the fifth Si layer.

II. SAMPLE PREPARATION

The Si(001) sample investigated at the Fritz-Haber Institut (FHI) in Berlin was lens shaped, which allowed one to compare the (001) orientation with orientations having miscuts towards all azimuths.[20] In this paper, however, only the (001) orientation is considered. The sample was prepared by cycles of argon ion sputtering (argon pressure, 3×10^{-5} mbar; ion energy 700 eV; ion current, 14 μA/cm^2) for about 15 min followed by annealing to 1530 K to remove residual contaminations of oxygen and water. After this treatment, the LEED pattern showed bright spots associated with a superposition of equal amounts of 2×1 and 1×2 domains and low background intensity. The most serious contamination of the Si(001) surface arises from the high susceptibility of this surface to water (the sticking probability is unity), which is inevitably present in the residual gas.[21] In order to study its influence, we recorded LEED *I-V* curves of two fractional and two integral order beams as a function of the water dose. It turned out that H_2O exposures of less than 0.2 L (1 Langmuir$=1.33\times10^{-6}$ mbar s) virtually do not alter the LEED *I-V* data. Since the experiments were performed in an UHV chamber under background pressure conditions of about 6×10^{-11} mbar, the actual measuring time of less than 1 h is short enough to allow for reliable experimental data. LEED *I-V* measurements were carried out at 120 K employing a video LEED system. Four integral-order and seven fractional-order (symmetry-inequivalent) beams were recorded at energies 30 and 220 eV (giving a cumulative energy range of 1510 eV). These measurements are referred to as FHI data in the following.

The second set of measurements were taken at the Institute of Crystallography at the University of Munich. This set of data is referred to as ICM data in the following. The sample was a commercially available wafer that was repeatedly etched in 40% HF and oxidized in 35% H_2O_2, each for 5 s and rinsed in triple distilled water. The final oxidation prior to mounting the sample into the UHV chamber was performed for 5 min. It was then sufficient to clean the sample in UHV by heating to 1170–1270 K for about 30 s. The sample exhibited then a bright LEED pattern with sharp spots and equal intensity of 1×2 and 2×1 superstructure spots. No impurities were detected in the Auger electron spectrum. The full LEED *I-V* data set was recorded first on a video tape within 10 min and (*ex situ*) subsequently the integrated LEED intensities dependent on the energy could be taken from the videotape employing a video LEED system; this procedure allows a fast data acquisition. After repeated cycles of cleaning by flashing the sample small amounts of carbon remained on the surface. If this kind of contamination occurred, the sample was replaced by a freshly prepared one. The data set used in the *I-V* analysis consist of five integral-order and seven fractional-order beams in the energy range 40–240 eV, providing a total energy range of 1500 eV. The sample temperature during the LEED measurements was 190 K.

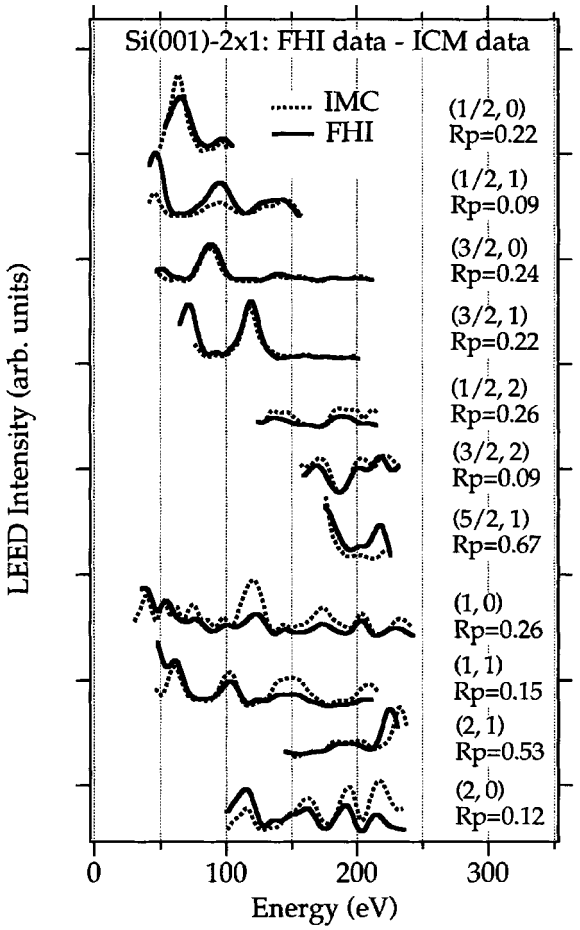

FIG. 1. Comparison of the experimental LEED data sets FHI and ICM. The overall Pendry *R* factor between these data sets is 0.25.

A comparison of both data sets is shown in Fig. 1. The data sets agree in the gross features of the *I-V* curves, but show also some discrepancies in the fine structure of some curves. The quantitative comparison of both data sets revealed an *r* factor of $R_P=0.25$, which is only moderate; for the definition of Pendry's *r* factor R_P the reader is referred to Ref. 22. The most striking discrepancies consist of an apparent shift of the peak at about 230 eV of the (2,1) beam and the different peak heights in most of the *I-V* curves, while the peak positions agree in most cases. It is conceivable that these differences are due to structural differences of both

samples resulting from the different preparation procedures. The FHI data set was taken from a sample that was prepared by Ar^+-ion bombardment and subsequent annealing. This procedure might be able to enhance the defect density on the surface. The tension introduced by surface defects may influence the local order and hence the dimer geometry. The FHI data set indicates clearly a faster decrease of the intensity with energy than the ICM data, although the ICM data were taken at a higher temperature. It therefore seems plausible to assign the differences in the experimental data sets to differing defect concentrations. Since even at low temperatures no well-ordered $c(2\times4)$ LEED pattern was observed, the defect concentration is quite high on both samples. Errors due to sample misalignment can be widely excluded since the I-V curves of symmetry-equivalent beams are almost identical. In principle, the differences in the relative intensities (from FHI to ICM) could also be due to different procedures for background subtraction and normalization. However, since the same LEED data acquisition system was used in both laboratories this explanation is not very convincing.

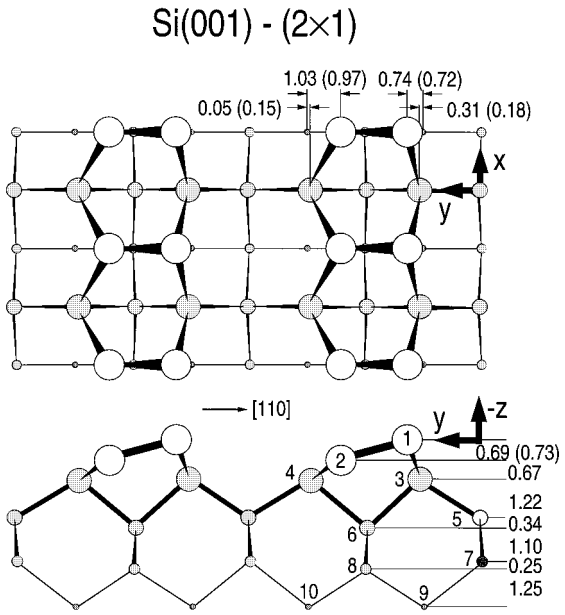

FIG. 2. Structure model and the main structural characteristics derived from the two LEED data sets. The numbers in parentheses are parameters obtained with the ICM data, while the other values are related to the FHI data. All parameter values are given in Angstrom units.

III. LEED I-V ANALYSIS AND DISCUSSION

Both LEED data sets were then fed into a full-dynamical LEED program that is equipped with a least-squares optimization scheme[23,24] in order to allow for the simultaneous refinement of structural parameters. The goodness of fit of calculated to experimental data was evaluated by the reliability factors R_P (Ref. 22) and the R_{de},[25] which also were the functionals to be minimized. The nonstructural parameters used in the multiple-scattering calculation were a band-structure crystal potential[26] and a maximum of nine phase shifts dependent on the energy. The real part of the inner potential was optimized in the analysis and led to an energy-independent value of 4.0 eV for the FHI data set, while the ICM data revealed an only slightly different value of 4.5 eV. For the ICM data set an energy-dependent inner potential led to a slight improvement of the best-fit R factors, while this was not the case with the FHI data set. The fit with an energy-dependent inner potential had virtually no influence on the structural parameters. The imaginary part of the inner potential (the optical potential) has been optimized as well by allowing constant values between 3 and 5 eV and also energy-dependent values $V_i=\text{const}(E+V_0)^{1/3}$ (eV), with const=0.7–0.9. The optical potential has a strong influence on the absolute intensities with the result that at high values of V_i the intensities at higher energies were too strongly damped. Little to no influence was found on the peak positions. The value taken in the final calculations was 3 eV and independent of energy. The layer-doubling scheme was used to calculate interlayer multiple scattering. A number of 80 symmetrically independent beams was used, well above the number sufficient to ensure convergence at 400 eV.

The structural parameters optimized in the fit procedure were the atomic coordinates in the top five layers including the dimer layer. The symmetry of the structure model was assumed to be pm according to the asymmetric dimer configuration and therefore allowing only the refinement of the y and z coordinates (cf. Fig. 2). In addition, the real part of the inner potential and the vibrational amplitudes in the topmost two layers were optimized leading to a total of 25 free

TABLE I. Structural parameters derived from the two data sets in comparison to results obtained by the *ab initio* calculation [Ref. 7(d)]. The first value in the table refers to the FHI data, the values in parentheses refer to the ICM data, and the values in square brackets refer to parameters obtained by density-functional theory calculations [Ref. 7(d)]. Fixed parameters are marked with an asterisk.

Si atom	x (Å)	y (Å)	z (Å)	Debye temperature (K)
1	1.92*	2.66, (2.63), [2.38]	0.00*	250, (231)±100
2	1.92*	4.73, (4.79), [4.53]	0.69, (0.73), [0.60]	295, (315)±100
3	0.00*	2.23, (2.10), [2.02]	1.43, (1.47), [1.35]	313, (291)±150
4	0.00*	5.71, (5.61), [5.61]	1.44, (1.47), [1.40]	877, (880)±300
5	0.00*	0.0*	2.63, (2.70), [2.62]	515, (636)±200
6	0.00*	3.84*	3.01, (3.06), [2.92]	643, (645)±200
7	1.92*	0.0*	4.08, (4.11), [4.02]	643, (646)±200
8	1.92*	3.84*	4.34, (4.37), [4.24]	640*
9	1.92*	1.84, (1.75), [1.88]	5.57, (5.61), [5.48]	640*
10	1.92*	5.83, (5.92), [5.67]	5.61, (5.65), [5.48]	640*

TABLE II. r factors reached with various best-fit model structures known from the literature on the basis of the FHI LEED data.

Model	R_p factor	r_{de} factor
Ref. 15	0.60	0.37
Ref. 16	0.78	0.49
Symmetric dimer including a twist (optimized)	0.42	0.37
Symmetric dimer without a twist (optimized)	0.48	0.37
Buckled dimer (this work)	0.26	0.26
Buckled dimer including twist ($\pm$0.1 Å) (optimized)	0.37	0.30

parameters. The optimum model was found by fitting first subsets of parameters independently followed by a simultaneous fit of all parameters in the final step. The relaxation in the sixth and deeper layers were found to be smaller than the error bars and hence to be set to the bulk values.

The analysis of both data sets led to very similar structural parameters. Given the differences in the experimental data, the best-fit structures agree remarkably well. The results are compiled in Table I and compared with parameters obtained by *ab initio* calculations.[7(d)] The structure model is schematically drawn in Fig. 2. The main structural features are the following. The topmost Si atoms are asymmetrically displaced along the [110] direction by 1.0 and 0.7 Å, respectively, so as to form the Si dimers. The dimer bond lengths derived from the FHI data are 2.20$\pm$0.08 Å and from the ICM data 2.28$\pm$0.08 Å. Both results agree within the error limits and show a slightly smaller bond length than that found in the Si bulk (2.35 Å), though this deviation is at the margin of the significance considering the level of agreement reached here. The Si dimer bond length found with LEED agrees well also with the value found by *ab initio* calculations such as 2.23 Å [Ref. 7d)] and 2.25 Å.[7(g)] This dimerization leads to small lateral (0.2–0.3 and 0.05–0.15 Å) and no detectable vertical displacements of Si atoms in the second layer. Both displacements have also been found with theory[7(d)] (cf. Table I). A more pronounced buckling as a result of a pairing in the second Si layer is observed with third-layer Si atoms, which amounts to 0.34$\pm$0.05 Å. This buckling in turn induces a buckling of the fourth layer by 0.25$\pm$0.07 Å. On symmetry grounds, a substantial buckling in the fifth Si layer is precluded, and due to the limited elastic mean free path of the electrons and the relatively large error bars of this analysis, we are not sensitive to distortions in even deeper Si layers though these parameters have been refined in the fit. Another important detail of this surface structure represents the tilting of the Si dimers. The vertical separation between the up and down atoms in the dimers is about 0.7 Å, which, together with its lateral asymmetry, provides bond lengths between the dimer atoms and the second-layer Si atoms directly underneath comparable with the bulk values. A twist of the Si dimers did not improve the agreement between theory and experiment. Rather, the introduction of a twist by more than 0.2 Å deteriorated the fit between experiment and theory markedly (cf. Table II). With the optimum structure shown in Fig. 2, the agreement between calculated and experimental LEED I-V curves is substantially improved as compared to previous LEED analyses. The final average r factors are $R_P = 0.26$ for the FHI data and 0.30 for the ICM data. The final level of agreement of experimental and calculated LEED I-V curves is demonstrated in Fig. 3 for the FHI data set and in Fig. 4 for the ICM data set.

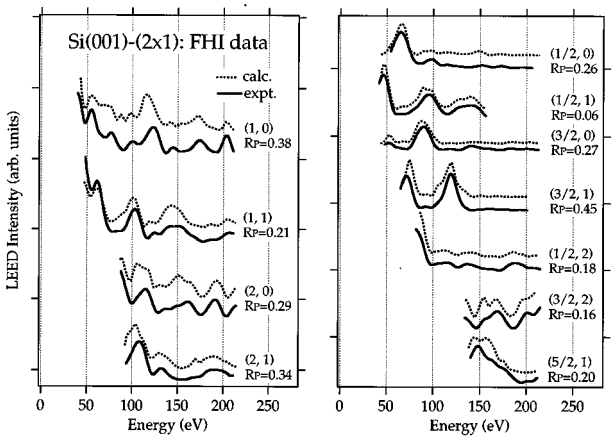

FIG. 3. Comparison of the best-fit LEED I-V curves with the experimental FHI data. The overall Pendry r factor is 0.26.

The differences in both analysis are mainly related to the different displacements in the second layer. The atoms in the second layer are drawn together by the dimer atoms, which in turn causes the buckling in the third layer. The pairing in the second layer amounts in both analyses to about 0.3$\pm$0.1 Å, but the lateral positions of both atoms differ by about 0.1 Å in the two data sets. All other parameters agree well within the error limits. The relaxations induced by the dimer have in both models the same direction and the relaxation in deeper layers is practically identical in both models. The observed differences are not unexpected in view of the differences in the experimental I-V curves.

Also remarkable is the agreement in the vibrational amplitudes (cf. Table I). Only isotropic vibrations were considered, which were refined in terms of Debye temperatures in the fit. Both analyses show a significant enhancement of the mean-square displacements of the topmost three atoms, although the specific values are subject to large uncertainties.

Additional points that need to be discussed are the sym-

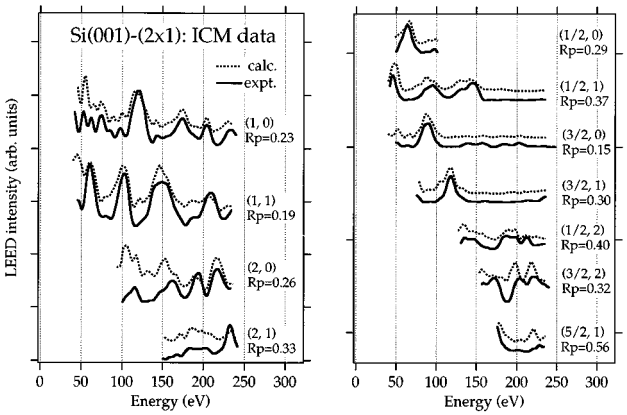

FIG. 4. Comparison of the best-fit LEED I-V curves with the experimental ICM data. The overall Pendry r factor is 0.30.

metry of the models and the averaging of the LEED intensities. The diffraction pattern exhibits $p4mm$ symmetry due to the simultaneous and equal presence of 2×1 and 1×2 domains from different terraces. The symmetry of the structure on a single terrace has been assumed to be pm. The models with twisted asymmetric dimers exhibit no symmetry, but these models could be excluded (cf. Table II). The Si dimers may exist as large ordered domains of aligned asymmetric dimers or as randomly distributed asymmetric dimers. The first model requires incoherent averaging with respect to $p2mm$, while the latter implies coherent averaging. In principle, the random-disordered model would require one to average the multiple-scattering paths by assuming an average of randomly oriented dimers around a given dimer. Since multiple scattering between dimers can be considered as negligibly small we have not performed this average, but performed instead an average of amplitudes calculated for the two possible ordered domains of aligned asymmetric dimers. Due to the presence of 2×1 and 1×2 domains from different terraces, the integral-order spots then have to be averaged incoherently with respect to $p4mm$. The I-V curves resulting from both procedures, coherent and incoherent averaging within one terrace, exhibited only small differences, much smaller than the differences in the experimental curves. Therefore we are not able to distinguish between the disorder model [which might be induced and stabilized by impurities as indicated by STM (Ref. 6)] and the alternative model of ordered domains [containing asymmetric dimers locally arranged with $c(2\times4)$ symmetry] on the basis of the present LEED data.

Next we compare calculated LEED I-V curves for the optimum structures (obtained by LEED) reported in the literature[13–16] with the experimental FHI LEED data. The resulting r factors are compiled in Table II. None of these optimum structures is able to fit the experimental FHI LEED data. Nevertheless, these early LEED analyses gave important clues about the Si(001)-2×1 structure. The dimerization of the top Si atoms was favored in all these studies. This kind of bonding was found to produce substantial strain in the top five atomic layers in accordance with theory.[27] The specific values of atomic displacements in deeper Si layers found in the LEED analysis by Yang, Jona, and Marcus[15] are practically identical to those found in our study. The main difference between this ''old'' LEED analysis and that presented here consists in the amplitude of the dimer buckling (0.7 Å), which is considerably larger than that reported earlier (0.4–0.5 Å). The dimer buckling of about 0.7 Å corresponds to a tilt angle of $19°\pm2°$ and agrees well with results found by recent theoretical studies.[7(d),7(h)]

From a recent surface x-ray-diffraction (SXRD) analysis[28] is was concluded that also the clean Ge(001)-2×1 surface constitutes surface dimers that are inclined out of the surface at an angle of about 15°; the separation between up and down atoms turned out to be 0.7 Å. A further study using the technique of x-ray standing waves was applied to a Ge-substituted dimer surface Ge/Si(001)-2×1.[29] The Ge-dimer buckling was found to be 0.55 Å, which is slightly smaller than that of the pure 2×1 phases on Si(001) and Ge(001). This slight deviation might be related to the heterogeneous composition of the top two semiconductor layers.

Recent transmission electron diffraction (TED) measurements revealed a tilting of the dimer axis against the in-plane surface by 5.5° for the Si(001)-2×1 structure,[30] a value that is at variance with that found here and also with recent total-energy calculations.[7] However, it is known that TED is relatively insensitive to displacements along the beam direction. Evidence for the presence of asymmetric dimer configurations on Si(001)-2×1 in the temperature range between 40 and 300 K has been provided by microscopic calculations of the optical properties.[31] Further support of asymmetric Si dimers was given by a previous SXRD study.[32] Both latter techniques, however, were not able to quantify the amplitude of this buckling. A very recent SXRD study of the Si(001)-(2×1) surface[33] found also the asymmetric Si dimer to be favored. While the lateral coordinates agree with the LEED results presented here, the vertical position of the Si dimer coordinates above the Si substrate deviate substantially by more than 0.2 Å. It is well known that SXRD is not very sensitive to vertical structure parameters since usually the momentum transfer perpendicular to the surface is rather small. This argument holds even more strongly as the SXRD analysis in Ref. 33 was based on a quite small data set with perpendicular momentum transfer reaching only values of $l=2$. For a detailed discussion of this kind of problem the reader is referred to a recent comparison of SXRD and LEED results of the Ge(111)-$\sqrt{3}\times\sqrt{3})R30°$-Au surface.[34]

IV. SUMMARY

In summary, we have presented a complete LEED structure analysis of the Si(001)-(2×1) surface. The topmost Si atoms are asymmetrically displaced by about 0.7 and 1.0 Å from the bulk positions in order to form Si dimers. The dimers are tilted by about $19°\pm2°$, i.e., the vertical separation between up and down atoms in the dimers is 0.72 Å. The Si-dimer bond length is 2.24 ± 0.08 Å (the averaged value found on the basis of two experimental LEED data sets), which is in agreement with theoretical studies.[7] The formation of Si dimers induces in turn distortions in deeper Si layers, most notably a buckling in the third and fourth layers by 0.34 and 0.25 Å, respectively, and a pairing in the second Si layer of 0.30 Å.

ACKNOWLEDGMENTS

We would like to thank Jaroslaw Dabrowski for supplying the Si coordinates found by density-functional theory ground-state calculations[7(d)] and Franco Jona for valuable discussions. The part of the analysis concerning the Institute of Crystallography has been financially supported by the DFG, through SFB 338.

*Author to whom correspondence should be addressed. Fax: ++49-30-8413-5106. Electronic address: over@hfi-berlin.mpg.de

[1] D. J. Chadi, Phys. Rev. Lett. **43**, 43 (1979).

[2] R. M. Tromp, R. J. Hamers, and J. E. Demuth, Phys. Rev. Lett. **55**, 1303 (1985).

[3] R. E. Schlier and H. E. Farnsworth, J. Chem. Phys. **30**, 917 (1959).

[4] J. J. Lander and J. Morrison, J. Chem. Phys. **37**, 729 (1962); T. Tabata, T. Aruga, and Y. Murata, Surf. Sci. **179**, L63 (1987).
[5] E. Landmark, C. J. Karlsson, Y.-C. Chao, and R. I. G. Uhrberg, Phys. Rev. Lett. **69**, 1588 (1992).
[6] R. A. Wolkow, Phys. Rev. Lett. **68**, 2636 (1992).
[7] (a) M. T. Yin and M. L. Cohen, Phys. Rev. B **24**, 2303 (1981); (b) N. Roberts and R. J. Needs, Surf. Sci. **236**, 112 (1990); (c) P. C. Weakliem, G. W. Smith, and E. A. Carter, *ibid.* **232**, L219 (1990); (d) J. Dabrowski and M. Scheffler, Appl. Surf. Sci. **56–58**, 15 (1992); (e) S. Tang, A. J. Freeman, and B. Delley, Phys. Rev. B **45**, 1776 (1992); (f) P. Krüger and J. Pollmann, *ibid.* **47**, 1898 (1993); (g) P. Krüger and J. Pollmann, Phys. Rev. Lett. **74**, 1155 (1995); (h) J. E. Northrup, Phys. Rev. B **47**, 10 032 (1993).
[8] J. Ihm, D. H. Lee, J. D. Joannopoulos, and J. J. Xiong, Phys. Rev. Lett. **51**, 1872 (1983).
[9] R. I. G. Uhrberg, G. V. Hansson, J. M. Nicholls, and S. A. Flodström, Phys. Rev. B **24**, 4684 (1981); R. D. Bringans, R. I. G. Uhrberg, M. A. Olmstead, and R. Z. Bachrach, *ibid.* **34**, 7447 (1986); F. J. Himpsel and Th. Fauster, J. Vac. Sci. Technol. A **2**, 815 (1983); P. Mårtensson, A. Cricenti, and G. V. Hansson, Phys. Rev. B **33**, 8855 (1986).
[10] R. J. Hamers and U. K. Köhler, J. Vac. Sci. Technol. A **7**, 2854 (1989).
[11] G. K. Wertheim, D. M. Riffe, J. E. Rowe, and P. H. Citrin, Phys. Rev. Lett. **67**, 1588 (1992).
[12] J. Gryko and R. E. Allen, Ultramicroscopy **42–44**, 793 (1992).
[13] S. Y. Tong and A. L. Maldonado, Surf. Sci. **78**, 459 (1978).
[14] S. J. White, D. C. Frost, and K. A. R. Mitchell, Solid State Commun. **42**, 763 (1982).
[15] W. S. Yang, F. Jona, and P. M. Marcus, Phys. Rev. B **28**, 2049 (1983).
[16] B. W. Holland, C. B. Duke, and A. Paton, Surf. Sci. **140**, L269 (1984).
[17] A. Ignatiev, F. Jona, M. Debe, D. E. Johnson, S. J. White, and D. P. Woodruff, J. Phys. C **10**, 1109 (1977).
[18] K. Müller, E. Lang, L. Hammer, W. Grimm, P. Heilmann, and K. Heinz, in *Determination of Surface Structure by LEED*, edited by P. M. Marcus and F. Jona (Plenum, New York, 1984), p. 483.
[19] M. Eckardt, H. Kleine, and D. Fick, Surf. Sci. **319**, 219 (1994).
[20] J. Wasserfall and W. Ranke, Surf. Sci. **315**, 237 (1994).
[21] E. Schröder-Bergen and W. Ranke, Surf. Sci. **236**, 103 (1990).
[22] J. B. Pendry, J. Phys. C **13**, 937 (1980).
[23] W. Moritz, J. Phys. C **17**, 353 (1983).
[24] G. Kleinle, W. Moritz, and G. Ertl, Surf. Sci. **238**, 119 (1990); H. Over, U. Ketterl, W. Moritz, and G. Ertl, Phys. Rev. B **46**, 15 438 (1992); M. Gierer, H. Over, and W. Moritz (unpublished).
[25] G. Kleinle, W. Moritz, D. L. Adams, and G. Ertl, Surf. Sci. **219**, L637 (1989).
[26] V. L. Moruzzi, J. F. Janak, and A. R. Williams, *Calculated Electronic Properties of Metals* (Pergamon, New York, 1978).
[27] A. Appelbaum and D. R. Hamann, Surf. Sci. **74**, 21 (1978).
[28] R. Rossmann, H. L. Meyerheim, V. Jahns, J. Wever, W. Moritz, D. Wolf, D. Dornisch, and H. Schulz, Surf. Sci. **279**, 199 (1992); X. Torrelles, H. A. van der Vegt, V. H. Etgens, P. Fajardo, J. Alvarez, and S. Ferrer, *ibid.* **364**, 242 (1996).
[29] E. Fontes, J. R. Patel, and F. Comin, Phys. Rev. Lett. **70**, 2790 (1993).
[30] G. Jayaram, P. Xu, and L. D. Marks, Phys. Rev. Lett. **71**, 3489 (1993).
[31] A. I. Shkrebtii and R. Del Sole, Phys. Rev. Lett. **70**, 2545 (1993).
[32] N. Jedrecy, M. Sauvage-Simkin, R. Inchaux, J. Massies, N. Greiser, and V. H. Etgens, Surf. Sci. **230**, 197 (1990).
[33] M. Takahasi, S. Nakatani, Y. Ito, T. Takahashi, X. W. Zhang, and M. Ando, Surf. Sci. **338**, L846 (1995).
[34] H. Over, C. P. Wang, and F. Jona, Phys. Rev. B **51**, 4231 (1995).